Graphene oxide affects soil bacterial and fungal diversity even at parts-per-trillion concentrations

Christian Forstner[a], Thomas G. Orton[b], Adam Skarshewski[a], Peng Wang[b,*], Peter M. Kopittke[b], Paul G. Dennis[a]#

[a]*School of Earth and Environmental Sciences, The University of Queensland, St Lucia, Brisbane, QLD 4072, Australia*

[b]*School of Agriculture and Food Sciences, The University of Queensland, St Lucia, Brisbane, QLD 4072, Australia*

Running Head: Graphene oxide affects soil microbial diversity

#Address correspondence to Paul G. Dennis, p.dennis@uq.edu.au

[*]Present address: *College of Resources and Environmental Sciences, Nanjing Agricultural University, Nanjing, China*.

Abstract

Graphene oxide (GO) is an oxidized form of graphene that is relatively cheap and easy to produce. This has heralded its widespread use in a range of industries, with its likelihood of release into the environment increasing accordingly. In pure culture, GO has been shown to influence bacteria and fungi, but its effects on environmental microbial communities remain poorly characterized, despite the important ecosystem services that these organisms underpin. Here, we characterized the effects of GO and graphite, over time and at three concentrations (1 ng, 1 µg and 1 mg kg dry soil^{-1}), on soil bacterial and fungal diversity using 16S rRNA and ITS2 gene amplicon sequencing. Graphite was included as a reference material as it is widely distributed in the environment. Neither GO or graphite had significant effects on the alpha diversity of microbial communities. The composition of bacterial and fungal communities, however, was significantly influenced by GO and graphite. These effects were equally apparent between doses and varied over time. Predicted KEGG pathways and fungal guild structures were not significantly influenced by the treatments. Our study demonstrates that GO can influence soil microbial diversity, even at parts-per-trillion concentration, which is equivalent to the rates of release predicted for similar nanomaterials such as carbon nanotubes.

Importance

Graphene oxide is a nanomaterial with broad and expanding industrial applications. Some evidence indicates that it can influence the growth of microorganisms, many of which support important ecosystem services, such as the provision of food and clean water. The amount of

graphene oxide currently entering soils is not known but is likely to be similar to other nanomaterials, such as carbon nanotubes (i.e. parts-per-trillion to parts-per-billion per year). In this study, we demonstrate that graphene oxide added to soil at these concentrations (or higher) can alter the composition of bacterial and fungal communities. Nonetheless, we found that these changes were of similar magnitude to those associated with the addition of graphite, which is common and occurs naturally in soils. Further research is recommended to determine whether the changes in microbial community composition that we have shown can be induced by graphene oxide, have deleterious consequences for soil health.

Keywords: phylogenetic marker gene sequencing, nanoparticles, graphene, microbial diversity, metagenomics, nanotechnology

Introduction

Graphene oxide (GO) is a nanomaterial with unique properties that has a wide-range of uses (1, 2). The environmental release of GO is predicted to increase along with the concomitant need to understand its potential ecological effects (3). Studies based on pure bacterial and fungal cultures indicate that GO can elicit both positive and negative effects on cell integrity and function. For example, GO can kill or suppress bacterial (4, 5) and fungal cultures (6, 7), by inducing oxidative stress (3, 4) or penetrating cell-walls and extracting phospholipids (8). On the other hand, some studies have shown that GO can act as a respiratory electron acceptor (9, 10) and promote the growth of bacterial cultures (11). These studies highlight that GO has the potential to affect soil microbial communities, which play fundamental roles in the provision of ecosystem goods and services (12, 13). Despite this, the impacts of GO on soil microbial diversity and function are poorly understood.

To the best of our knowledge, there are only four previous studies that have directly investigated the effects of GO on soil microbial communities (14–17). The first, focused exclusively on soil microbial biomass and enzyme activities (15). It revealed significant, but temporary, effects on the activities of xylosidase, β-1,4-N-acetyl glucosaminidase, and acid phosphatase, and no effects on microbial biomass (15). The second study aimed to compare the diversity of bacterial communities in control and GO-amended soils using phylogenetic marker gene sequencing (17). The authors claimed that GO increased soil bacterial diversity and altered community composition (17). Nonetheless, as highlighted by Forstner *et al*. (18), their claims were unjustified as their study lacked replication within treatments (n=1), and did not account for

differences in the numbers of sequences per sample when comparing the numbers of taxa present. The third study investigated the effects of GO on microbial enzyme activities and bacterial diversity in cadmium contaminated soil (14). It revealed that the activities of catalase and dehydrogenase increased, while that of urease decreased in response to GO (14). Furthermore, the composition of bacterial communities, but not their diversity, appeared to be influenced by GO, although no statistical support for this was provided (14). Lastly, the fourth study focused on the effects of silver-GO nanocomposites on soil bacterial communities, but included a GO treatment (16). Unfortunately, this GO treatment was not compared to a water-only control; therefore, it was not possible to isolate GO effects from those attributable to Ag (16).

Importantly, all previous studies applied GO at doses that are considerably higher than those likely to be encountered in the environment. The main routes of entry for many nanomaterials into the environment are thought to be wastewater treatment and landfill (19–21). While data are not available for GO, models estimate that 3.7-7.1 ng and 0.8-1.6 µg of carbon nanotubes (CNTs) kg soil^{-1} enter European natural and sludge-amended soils every year (21). Model estimates for the rate of release of other nanomaterials into soils (nanosilver, nano-ZnO and fullerenes) are similar (21). Chung *et al*. (15) applied 0.1-1.0 g GO kg soil^{-1}, while Xiong *et al*. (14) and Du *et al*. (17) applied 1.0-2.0 g and 5 g GO kg soil^{-1}, respectively. These doses are equivalent to between 62.5 thousand and 1.25 billion times the estimated annual rate of accumulation for CNTs (21). Hence, the effects of GO on soil microbial diversity are poorly understood, particularly at concentrations approximating those deemed realistic for similar nanomaterials. In addition, as previous studies have only considered bacterial communities, the effects of GO on other important groups of soil organisms, such as fungi, are not known.

Finally, when characterizing the effects of nanomaterials on soil microbial diversity it is important to include reference materials that provide a context with which to interpret changes (22). For example, while a significant shift in microbial diversity may be observed in response to a nanomaterial, the magnitude of such a change may be small in comparison to those associated with material that are already widely distributed in the environment. Clearly, therefore, this information is essential for the development of appropriate policy frameworks for the safe and sustainable use of nanomaterials. Despite this, such reference materials were not included in any of the previous studies concerning the effects of GO on soil microbial communities (14–17).

In this study, we investigated the effects of one-off applications of GO and graphite on soil bacterial and fungal diversity using high-throughput phylogenetic marker gene sequencing. Graphite was included as a reference compound as it chemically similar to GO, without being classed as a nanomaterial, and is widely distributed in the environment. GO and graphite were applied at concentrations ranging from parts per trillion to parts per million (1 ng, 1 µg and 1 mg GO kg soil^{-1}) representing environmentally relevant low, high and extremely high rates of release based on those predicted for CNTs (21). All treatments were replicated three times and communities were characterized 7, 14 and 30 days after application.

Results

Alpha diversity of soil microbial communities.

The numbers of observed (Sobs) and predicted (Chao1) bacterial and fungal taxa, as well as the phylogenetic diversity of bacterial communities (Faith's PD), were not significantly influenced by any of the GO or graphite treatments relative to the controls throughout the experiment (Fig. 1, S1 and S2).

Soil bacterial community composition and predicted metagenomes.

Relative to the controls, the composition of soil bacterial communities was significantly influenced by the addition of GO and graphite, and these effects differed over time ($P < 0.001$). Effects were observed for both materials at all doses except for the low GO dose on day 14 (Tables 1 and S1). Albeit significant, there was not a consistent direction of change in bacterial community composition with increasing GO or graphite dose (Fig. 2). Bacterial community composition differed significantly between all GO and graphite treatments (Table S2).

Bacterial communities were dominated by representatives of the Acidobacteria, Actinobacteria, Armatimonadetes, Bacteriodetes, Candidatus Berkelbacteria, Chlamydiae, Chlorobi, Chloroflexi, Fibrobacteres, Firmicutes, Gemmatimonadetes, Microgenomates, Planctomycetes and Proteobacteria, Saccharibacteria, and Verrucomicrobia (Fig. S3).

The 100 OTUs that were most strongly associated with differences in community composition between treatments were obtained from the multivariate GLMs and assessed independently using

univariate GLM models. Of these 49 were found to differ significantly from the control in at least one treatment combination after Benjamini-Hochberg correction for multiple comparisons (Fig. 3). Four OTUs responded exclusively to GO: a member of the *Tepidisphaeraceae* (OTU81, Planctomycetes) and an *Oligoflexales* (OTU363, Deltaproteobacteria) that increased in relative abundance in the presence of GO; a Ktedonobacteria (OTU1084, Chloroflexi) population which declined; and a representative of the *Acidobacteriaceae* (OTU2196, Acidobacteria), which increased at some doses but declined at others (Fig. 3). An additional 30 OTUs, representing a broad-range of phyla, responded to both GO and graphite (Fig. 3). The remaining 15 OTUs, again of broad phylogenetic coverage, responded exclusively to graphite (Fig. 3).

Metagenomes corresponding to the taxa present were inferred using Phylogenetic Investigation of Communities by Reconstruction of Unobserved States (PICRUSt) (23), which produced tables of predicted molecular functions represented as Kyoto Encyclopedia of Genes and Genomes (KEGG) (24) functional orthologs (KOs). Based on these KO profiles, the Human Microbiome Projects' Unified Metabolic Analysis Network 2 (HUMAnN2) pipeline (25) was used to assess the abundance of KEGG functional modules and pathways. GO and graphite did not significantly influence the abundance of the predicted KEGG functional modules or pathways. When considered independently, however, the structure of predicted KO profiles was significantly influenced by treatment ($P < 0.001$) and these effects did not differ over time. Post-hoc analyses revealed that the medium GO, and low and medium graphite treatments differed relative to the controls (Table S3). Of the significantly affected KOs, 31 responded exclusively to GO, and 66 responded to both GO and graphite (Fig. S4). Most of these KOs were associated with cellular

maintenance and growth, such as ribosomal subunits, transporter proteins and amino acid synthesis (Fig. S4).

Soil fungal community composition and predicted guild structure.

Relative to the controls, the composition of soil fungal communities was significantly influenced by the addition of GO and graphite at all doses ($P = 0.001$), and these treatment effects did not differ significantly over time (Tables 2 and S4). As observed for bacteria, there was not a consistent direction of change in the composition of fungal communities with increasing GO or graphite dose (Fig. 4). Fungal community composition differed significantly between all GO and graphite treatments (Table S5).

Soil fungal communities were dominated by representatives of the Ascomycota, Basidiomycota, Mortierellomycota, Mucoromycota and Chytridiomycota (Fig. S5). As for the bacteria, the fungal OTUs that were most strongly associated with differences in community composition between treatments were obtained from the multivariate GLMs and assessed independently using univariate GLM models. Of these, 16 OTUs were found to differ significantly from the control in at least one treatment combination after Benjamini-Hochberg correction for multiple comparisons (Fig. 5).

No fungal OTUs responded exclusively to GO; however, 10 responded to both GO and graphite (Fig. 5). In all cases the direction of response for these OTUs was the same for GO as it was for graphite. Four of these OTUs were negatively associated with GO and graphite *viz.* a *Goidanichiella sphaerospora* (OTU 10), a *Pleosporales* (OTU 87), a *Kendrickiella phycomyces*

(OTU 16) and a *Hendersonia* (OTU 41) population (Fig. 5). In contrast, the relative abundances of six OTUs were positively associated with GO and graphite: an *Arthrobotrys musiformis* (OTU 17), a *Trichoderma virens* (OTU 136), a *Saitozyma podzolica* (OTU 62), a *Ceratocystidaceae* (OTU 3), a *Clonostachys candelabrum* (OTU 25), and a *Fusarium* (OTU 422) population (Fig. 5). The remaining six OTUs responded exclusively to graphite with two decreasing (OTUs 85 and 39) and four increasing (OTUs 53, 56, 75, and 58) in relative abundance, respectively (Fig. 5).

Functional guilds were assigned to 63% of fungal OTUs using FUNGuild (26). Multivariate GLM analysis indicated that fungal guild structure was stable over time and was not significantly influenced by the treatments.

Discussion

Our study demonstrates that GO can significantly alter the composition of soil bacterial and fungal communities at loading rates equal to, and beyond, those estimated for the annual accumulation of other nanomaterials (e.g. carbon nanotubes, nanosilver, nano-TiO_2 and nano-ZnO) in soils (21). Nonetheless, our reference material, graphite, also led to significant shifts in community composition, and these were of similar magnitude to those observed for GO, albeit with some differences in the taxa affected. Despite these changes, we observed no significant effects of GO or graphite on alpha diversity, predicted bacterial functional gene pathways and modules, or predicted fungal guild structure. Hence, our study did not provide evidence indicating that GO-induced shifts in community composition affect soil ecosystem functioning. It

is important to note, however, that while our approach enabled robust assessment of the impacts of GO on microbial diversity, functional inference from phylogenetic marker gene sequences may poorly represent the attributes of the populations present (27).

Of the four previous studies that investigated the effects of GO on soil microbial communities (14–17), three considered bacterial diversity (14, 16, 17) and two measured microbial enzyme activities (14, 15). In all cases, the results for bacterial diversity were inconclusive due to a lack of replication (17), no treatment controls (16) or statistical analyses (14, 17). The activities of several enzymes, however, were significantly, albeit only temporally, influenced by GO addition (14, 15), suggesting that GO has at least some potential to influence soil ecosystem functioning. Nonetheless, all previous studies have focused on the effects of extremely high GO doses – equivalent to between 62.5 thousand and 1.25 billion times the estimated annual rate of accumulation for CNTs (21). It could be argued, therefore, that smaller doses would have lesser effects on microbial communities.

Interestingly, our study highlights that the magnitude of community compositional changes observed did not increase with the amount of material applied, or decrease over time. This indicates that even low GO doses (i.e. parts per trillion to parts per billion) can induce community compositional changes that persist beyond 30 days. We speculate that this lack of ‘linear’ dose-response to GO is related to an agglomeration of GO sheets (28), covering of sheets with other materials (29), or interactions with components of the soil matrix (30), such as clays which possess a large surface area, capable of binding and immobilizing GO sheets (31). These interactions could strongly influence the number of GO sheets that interact with soil microbes

and significantly alter the properties that they exhibit as pristine nanoparticles. For example, culture-based studies have demonstrated that the edges of GO sheets can cut and destructively extract phospholipids (8, 32) from microbial cell membranes. This destructive property of GO is likely to be undermined by interactions that would reduce the number of ‘sharp’ edges (4, 5).

While there were significant differences in community composition between GO and graphite amended soils, the majority of OTUs that discriminated between treatments, responded in a similar manner to both materials. For example, 61% and 63% of discriminating bacterial and fungal taxa, respectively, responded to both GO and graphite. In contrast, just 8% of discriminating bacterial taxa, and no fungal taxa, responded exclusively to GO; while 31% and 38% of discriminating bacterial and fungal taxa, respectively, responded exclusively to graphite. In general, there were roughly equal numbers of positive and negative responses for taxa responding to GO and/or graphite. This observation corroborates pure culture studies, which report both positive and negative effects of GO on bacterial and fungal isolates (3–11). One of the ways in which GO may benefit microbes is by acting as a terminal electron acceptor (9, 10); however, we did not find evidence that respiratory pathways were affected by GO and did not detect any taxa that are well-known to perform extracellular electron transfer. In summary, fewer populations responded exclusively to GO than to graphite; most responded to both materials; and the numbers of positively and negatively affected taxa were about equal.

Despite lacking replication and/or statistical analyses, previous studies that investigated the effects of GO on soil microbial diversity have drawn attention to apparent differences in the relative abundances of ecologically significant taxa, such as those involved in nitrogen cycling.

Xiong *et al.* (14), for example, reported an increase in the relative abundance of *Rhizobiales* populations and decreases in the relative abundances of *Rhodospirrillaeceae* and *Nitrospirae*. In our study, just one *Rhizobiales* (OTU 195) population was affected by GO addition, and this effect manifested as a decrease in its relative abundance at 7 days, followed by an increase after 14 days. Among the *Rhodospirrilaeceae*, we observed an increase in the relative abundance of OTU 1929, and a decrease in the relative abundance of OTU 819 in response to GO addition (Fig. 3). We did not detect any significant changes in the relative abundances of members of the *Nitrospirae* in response to GO or graphite. To the best of our knowledge, the effects of GO on soil fungal communities have not been previously examined. In pure culture, GO has been shown to suppress the growth of *Fusarium oxysporum*, a species known to contain multiple plant pathogens (6). Despite being present within our inventories, we did not detect significant effects of GO on this species; however, the relative abundance of an unclassified relative within the same genus (OTU 422) was observed to increase in response to both GO and graphite addition (Fig. 5).

Conclusion

As the use of GO increases, its release into the environment will rise. Our study demonstrates that that GO influences bacterial and fungal community composition, even at parts per trillion concentrations. In light of this finding, it is important that future studies examine whether GO-induced changes in microbial diversity are likely to undermine the provision of soil ecosystem goods and services.

Methods

Experimental design.

The soil used in this study is classified as a Kandosol according to the Australian Soil Classification (33), or an Ultisol according to the USDA Soil Taxonomy (34) and has been described in our previous work (see Table S1 from Wang *et al*. (35)). Briefly, the soil was collected at a depth of 0−20 cm from a pineapple (*Ananas comosus*) farm in Queensland, Australia. The soil had a sandy loam texture, pH of 5.4 (1:5 soil/water), conductivity of 0.1 dS/m (1:5 soil/water), and total organic Carbon content of 1.1%. Approximately 11 kg of fresh soil was passed through a 2 mm sieve and then split into seven c. 1.6 kg sub-samples to which the treatments were applied. Graphene oxide (Aldrich Chemistry, CAT: 763705, Lot# MKBQ8029V) and graphite (Sigma Aldrich, CAT:282863, size <20 μm) were applied to soils at rates of 1 ng, 1 μg and 1 mg kg dry soil^{-1} using a fine mist sprayer and thoroughly homogenized by mechanical mixing. In brief, either the GO or graphite was dispersed into deionized water at a volume that resulted in the soil being adjusted to 50% water holding capacity (WHC). The solution was then sprayed on the soil prior to mechanical mixing. These three rates were selected to represent environmentally relevant, high and extremely high concentrations based on release rates predicted for CNTs (21). Soils in the control treatments were sprayed with an equal quantity of deionized water only. Three replicate 500 g samples of each treatment were placed into 1 L plastic containers with lids that facilitated gas exchange. This yielded 21 containers that were incubated for 30 days in the dark at 25ºC, with the humidity maintained at 80% in order to keep the soils at the same WHC throughout the experimental period.

Soil sampling and DNA extraction.

Soil cores, of approximately 25 g, were collected from each experimental unit after 7, 14 and 30 days using sterile 50 ml plastic tubes, and immediately transferred to -80ºC storage. DNA was extracted from 250 mg of thawed soil using the Power Soil DNA Isolation kit (MO BIO Laboratories, Carlsbad, CA) according to the manufacturers' instructions.

PCR amplification and sequencing of phylogenetic marker genes.

Universal bacterial 16S rRNA genes were amplified by polymerase chain reaction (PCR) using the primers 926F (5'-AAA CTY AAA KGA ATT GRC GG-3') (36) and 1392wR (5'-ACG GGC GGT GWG TRC-3') (36). Fungal ITS2 regions were PCR amplified using the primers gITS7F (5'- GTG ART CAT CGA RTC TTT G -3') (37) and ITS4R (5'- TCC TCC GCT TAT TGA TAT GC -3') (38). For both groups, the forward and reverse primers were modified on the 5' end to contain the Illumina overhang adapter for compatibility with the i5 and i7 Nextera XT indices, respectively. PCRs were performed with 1.5 µl template DNA, in 1X PCR Buffer minus Mg^{2+} (Invitrogen), 100 µM of each of the dNTPs (Invitrogen), 300 µM of $MgCl_2$ (Invitrogen), 0.625 U Taq DNA Polymerase (Invitrogen), and 250 µM of each primer, made up to a total volume of 25 µl with molecular biology grade water. Thermocycling conditions were as follows: 94°C for 3 minutes; then 35 cycles of 94°C for 45 seconds, 55°C for 30 seconds, 72°C for 1 minute 30 seconds; followed by 72°C for 10 minutes. Amplifications were performed using a Veriti® 96-well Thermocycler (Applied Biosystems). PCR success was determined by gel electrophoresis, which also facilitated visual confirmation of amplicon size and quality.

Amplicons were purified using AMPure magnetic beads (Agencourt) and subjected to dual indexing using the Nextera XT Index Kit (Illumina) as per the manufacturer's instructions. Indexed amplicons were purified using AMPure XP beads and then quantified using a PicoGreen dsDNA Quantification Kit (Invitrogen). Equal concentrations of each sample were pooled and sequenced on an Illumina MiSeq at The University of Queensland's Institute for Molecular Biosciences (UQ, IMB) using 30% PhiX Control v3 (Illumina) and a MiSeq Reagent Kit v3 (600 cycle; Illumina) according the manufacturer's instructions.

Processing of sequence data.

Data were analyzed using a modified UPARSE pipeline (39). For both datasets, analyses were performed using the forward reads only. For 16S rDNA sequences, USEARCH (v10.0.240) (40) was used to perform the following steps: 1) primers were removed and the residual sequences were trimmed to 250 bp using fastx_truncate; 2) high-quality sequences were identified using fastq_filter by discarding reads with greater than one expected error (-fastq_maxee=1); 3) duplicate sequences were removed using fastx_uniques; 4) sequences were clustered at 97% similarity into operational taxonomic units (OTU) and potential chimeras were identified and removed using cluster_otus; and 5) an OTU table was generated using otutab with default parameters from the pre-trimmed reads and the OTU representative sequences. For the ITS data, ITSx v1.0.11 (41) was used to identify and extract fungal ITS2 sequences. Chimeric ITS2 sequences were identified and removed using the uchime2_ref command of USEARCH and the UNITE database (v7.2 - 2017.10.10) (42). ITS2 sequences were then clustered at 97% similarity into operational taxonomic units (OTU) and an OTU table was generated using the otutab command of USEARCH with default parameters. SILVA SSU (v128) (43) and UNITE (v7.2-

2017.10.10) (42) taxonomy was assigned to the 16S and ITS sequences, respectively, using BLASTN (v2.3.0+) (44) within the feature classifier of QIIME2 (v2017.9) (45). The 16S OTU table was then filtered to remove OTUs classified as chloroplasts, mitochondria, archaea or eukaryotes using the BIOM (46) tool suite. For 16S, de-novo multiple sequence alignments of the representative OTU sequences were generated using MAFFT (v7.221) (47) and masked with the alignment mask command of QIIME2. The masked alignment was used to generate a midpoint-rooted phylogenetic tree using FastTree (v2.1.9) (48) in QIIME2. OTU tables were rarefied to 4850 and 1150 sequences per sample for 16S and ITS, respectively. The mean numbers of observed (Sobs) and predicted (Chao1) OTUs were calculated using QIIME2 for both bacteria and fungi. For bacteria, we also calculated Faith's phylogenetic diversity index (Faith's PD) (49) using QIIME2.

For 16S, metagenomes corresponding to the taxa listed in the rarefied OTU table were inferred using PICRUSt (v1.1.2) (23), which produced tables of predicted molecular functions represented as KEGG (24) functional orthologs (KOs). The HUMAnN2 pipeline (25) was then used to assess the abundance of KEGG functional modules and pathways in each sample. For fungi, we used FUNGuild (v1.1) to parse taxa in the rarefied OTU table into functional guilds based on their taxonomic assignments (26). As recommended by the FUNGuild development team (26), we excluded taxa for which the functional guild assignment was of low ("possible") confidence.

Statistical analyses.

For statistical analyses, we defined Treatment as the combination of applied substance (none for the control, GO or graphite) and applied dose (1 ng, 1 µg or 1 mg kg dry soil^{-1}). Hence,

Treatment was defined as a categorical variable with seven classes. In order to determine whether the GO and graphite treatments significantly affected the alpha diversity metrics, we used a linear mixed-effects model approach (50). Treatment (as defined above) and Day, as well as their interaction, were treated as fixed effects, and soil containers (samples) were treated as a random effect to account for the repeated measures. F-tests were applied to assess significance ($P<0.05$), and were implemented in R using the lme4 (51) and lmerTest (52) packages.

Differences in the relative abundances of taxa between samples (beta diversity), and the inferred functional profiles were assessed using multivariate generalized linear models using a negative binomial distribution (53). The significance of differences in community composition was determined by comparing the sum-of-likelihood test statistics for the alternative statistical models via a resampling method (54) that accounted for the correlation between species and the correlation within the repeated measures taken from the same sample container. These comparisons were implemented in R using the mvabund package (54). Taxa whose maximum relative abundance was less than 0.1% for bacteria or 0.4% for fungi were disregarded before statistical analysis. Where an interactive effect of Treatment and Day was significant, post-hoc analyses were undertaken to investigate which Treatments differed on what Days. Where no interactive effect was found, but a main effect of Treatment was, post-hoc analyses focused on which Treatments differed from one another. The Benjamini-Hochberg correction was applied to all post-hoc tests.

Data availability.

All sequences have been deposited to the Sequence Read Archive (SRA) under BioProject accession number PRJNA515098 (55).

Acknowledgements

The authors gratefully acknowledge financial support from The University of Queensland for an Early Career Researcher Award to PGD. CF gratefully acknowledges funding from the Australian Government's Department of Education and Training in the form of an Australian Government Research Training Program Scholarship administered by The University of Queensland. PMK is the recipient of an Australian Research Council (ARC) Future Fellowship (ARC FT120100277).

Declaration of interest

The authors report that they have no conflicts of interest.

Author contributions

PGD, PMK and PW conceived the study. CF, PW and PGD set up the soil incubations. CF performed the experiments. TGO, CF, AS and PGD analyzed the data. PGD and CF wrote the manuscript with input from the other authors.

References

1. Novoselov KS, Fal′ko VI, Colombo L, Gellert PR, Schwab MG, Kim K. 2012. A roadmap for graphene. Nature 490:192–200.

2. Yoo BM, Shin HJ, Yoon HW, Park HB. 2014. Graphene and graphene oxide and their uses in barrier polymers. J Appl Polym Sci 131:1–23.

3. Ahmed F, Rodrigues DF. 2013. Investigation of acute effects of graphene oxide on wastewater microbial community: A case study. J Hazard Mater 256–257:33–39.

4. Liu S, Zeng TH, Hofmann M, Burcombe E, Wei J, Jiang R, Kong J, Chen Y. 2011. Antibacterial activity of graphite, graphite oxide, graphene oxide, and reduced graphene oxide: Membrane and oxidative stress. ACS Nano 5:6971–6980.

5. Akhavan O, Ghaderi E. 2010. Toxicity of graphene and graphene oxide nanowalls against bacteria. ACS Nano 4:5731–5736.

6. Chen J, Peng H, Wang X, Shao F, Yuan Z, Han H. 2014. Graphene oxide exhibits broad-spectrum antimicrobial activity against bacterial phytopathogens and fungal conidia by intertwining and membrane perturbation. Nanoscale 6:1879–1889.

7. Li X, Li F, Gao Z, Fang L. 2015. Toxicology of graphene oxide nanosheets against *Paecilomyces catenlannulatus*. Bull Environ Contam Toxicol 95:25–30.

8. Tu Y, Lv M, Xiu P, Huynh T, Zhang M, Castelli M, Liu Z, Huang Q, Fan C, Fang H, Zhou R. 2013. Destructive extraction of phospholipids from *Escherichia coli* membranes by graphene nanosheets. Nat Nanotechnol 8:594–601.

9. Salas EC, Sun Z, Lüttge A, Tour JM. 2010. Reduction of graphene oxide via bacterial respiration. ACS Nano 4:4852–4856.

10. Wang G, Qian F, Saltikov CW, Jiao Y, Li Y. 2011. Microbial reduction of graphene oxide by *Shewanella*. Nano Res 4:563–570.

11. Ruiz ON, Fernando KAS, Wang B, Brown NA, Luo PG, McNamara ND, Vangsness M, Sun Y-P, Bunker CE. 2011. Graphene oxide: A nonspecific enhancer of cellular growth. ACS Nano 5:8100–8107.

12. Wagg C, Bender SF, Widmer F, van der Heijden MGA. 2014. Soil biodiversity and soil community composition determine ecosystem multifunctionality. Proc Natl Acad Sci U S A 111:5266–5270.

13. Bardgett RD, van der Putten WH. 2014. Belowground biodiversity and ecosystem functioning. Nature 515:505–511.

14. Xiong T, Yuan X, Wang H, Leng L, Li H, Wu Z, Jiang L, Xu R, Zeng G. 2018. Implication of graphene oxide in Cd-contaminated soil: A case study of bacterial communities. J Environ Manage 205:99–106.

15. Chung H, Kim MJ, Ko K, Kim JH, Kwon H, Hong I, Park N, Lee SW, Kim W. 2015. Effects of graphene oxides on soil enzyme activity and microbial biomass. Sci Total Environ 514:307–313.

16. Kim MJ, Ko D, Ko K, Kim D, Lee JY, Woo SM, Kim W, Chung H. 2018. Effects of silver-graphene oxide nanocomposites on soil microbial communities. J Hazard Mater 346:93–102.

17. Du J, Hu X, Zhou Q. 2015. Graphene oxide regulates the bacterial community and exhibits property changes in soil. RSC Adv 5:27009–27017.

18. Forstner C, Wang P, Kopittke PM, Dennis PG. 2016. Comment on “Graphene oxide regulates the bacterial community and exhibits property changes in soil” by J. Du, X. Hu and Q. Zhou, RSC Advances, 2015, 5, 27009. RSC Adv 6:51203–51204.

19. Gottschalk F, Sonderer T, Scholz RW, Nowack B. 2009. Modeled environmental concentrations of engineered nanomaterials (TiO2, ZnO, Ag, CNT, fullerenes) for different regions. Environ Sci Technol 43:9216–9222.

20. Mueller NC, Nowack B. 2008. Exposure modeling of engineered nanoparticles in the environment. Environ Sci Technol 42:4447–4453.

21. Sun TY, Gottschalk F, Hungerbühler K, Nowack B. 2014. Comprehensive probabilistic modelling of environmental emissions of engineered nanomaterials. Environ Pollut 185:69–76.

22. Petersen EJ. 2015. Control experiments to avoid artifacts and misinterpretations in nanoecotoxicology testing. NIST Spec Publ 1200-11:1–7.

23. Langille MGI, Zaneveld J, Caporaso JG, McDonald D, Knights D, Reyes JA, Clemente JC, Burkepile DE, Vega Thurber RL, Knight R, Beiko RG, Huttenhower C. 2013. Predictive functional profiling of microbial communities using 16S rRNA marker gene sequences. Nat Biotechnol 31:814–821.

24. Kanehisa M, Goto S. 2000. KEGG: Kyoto encyclopedia of genes and genomes. Nucleic Acids Res 28:27–30.

25. Franzosa EA, McIver LJ, Rahnavard G, Thompson LR, Schirmer M, Weingart G, Schwarzberg Lipson K, Knight R, Caporaso JG, Segata N, Huttenhower C. 2018. Species-level functional profiling of metagenomes and metatranscriptomes. Nat Methods 15:962–968.

26. Nguyen NH, Song Z, Bates ST, Branco S, Tedersoo L, Menke J, Schilling JS, Kennedy PG. 2016. FUNGuild: An open annotation tool for parsing fungal community datasets by ecological guild. Fungal Ecol 20:241–248.

27. Béjà O, Koonin EV, Aravind L, Taylor LT, Seitz H, Stein JL, Bensen DC, Feldman RA, Swanson RV, DeLong EF. 2002. Comparative genomic analysis of archaeal genotypic variants in a single population and in two different oceanic provinces. Appl Environ Microbiol 68:335–45.

28. Dreyer DR, Park S, Bielawski CW, Ruoff RS. 2010. The chemistry of graphene oxide. Chem Soc Rev 39:228–240.

29. Hui L, Piao JG, Auletta J, Hu K, Zhu Y, Meyer T, Liu H, Yang L. 2014. Availability of the basal planes of graphene oxide determines whether it is antibacterial. ACS Appl Mater Interfaces 6:13183–13190.

30. Chen L, Yang S, Liu Y, Mo M, Guan X, Huang L, Sun C, Yang ST, Chang XL. 2018. Toxicity of graphene oxide to naked oats (*Avena sativa* L.) in hydroponic and soil cultures. RSC Adv 8:15336–15343.

31. Lu T, Xia T, Qi Y, Zhang C, Chen W. 2017. Effects of clay minerals on transport of graphene oxide in saturated porous media. Environ Toxicol Chem 36:655–660.

32. Lu X, Feng X, Werber JR, Chu C, Zucker I, Kim JH, Osuji CO, Elimelech M. 2017. Enhanced antibacterial activity through the controlled alignment of graphene oxide nanosheets. Proc Natl Acad Sci U S A E9793–E9801.

33. Isbell RF. 2002. The australian soil classification (Revised ed.). CSIRO Publishing, Collingwood, Victoria.

34. Soil Survey Staff. 2014. Keys to soil taxonomy, 12th ed. USDA -Natural Resources Conservation Service, Washington, DC.

35. Wang P, Menzies NW, Dennis PG, Guo J, Forstner C, Sekine R, Lombi E, Kappen P, Bertsch PM, Kopittke PM. 2016. Silver nanoparticles entering soils via the wastewater–sludge–soil pathway pose low risk to plants but elevated Cl concentrations increase Ag bioavailability. Environ Sci Technol 50:8274–8281.

36. Engelbrektson A, Kunin V, Wrighton KC, Zvenigorodsky N, Chen F, Ochman H, Hugenholtz P. 2010. Experimental factors affecting PCR-based estimates of microbial species richness and evenness. ISME J 4:642–647.

37. Ihrmark K, Bödeker ITM, Cruz-Martinez K, Friberg H, Kubartova A, Schenck J, Strid Y, Stenlid J, Brandström-Durling M, Clemmensen KE, Lindahl BD. 2012. New primers to amplify the fungal ITS2 region - evaluation by 454-sequencing of artificial and natural communities. FEMS Microbiol Ecol 82:666–677.

38. White TJ, Bruns T, Lee S, Taylor JW. 1990. Amplification and direct sequencing of fungal ribosomal RNA genes for phylogenetics., p. 315–322. In Innis, MA, Gelfand, DH, Sninsky, JJ, White, TJ (eds.), PCR protocols: A guide to methods and applications. Academic Press, New York.

39. Edgar RC. 2013. UPARSE: Highly accurate OTU sequences from microbial amplicon reads. Nat Methods 10:996–998.

40. Edgar RC. 2010. Search and clustering orders of magnitude faster than BLAST. Bioinformatics 26:2460–2461.

41. Bengtsson-Palme J, Ryberg M, Hartmann M, Branco S, Wang Z, Godhe A, De Wit P, Sánchez-García M, Ebersberger I, de Sousa F, Amend AS, Jumpponen A, Unterseher M, Kristiansson E, Abarenkov K, Bertrand YJK, Sanli K, Eriksson KM, Vik U, Veldre V, Nilsson RH. 2013. Improved software detection and extraction of ITS1 and ITS2 from ribosomal ITS sequences of fungi and other eukaryotes for analysis of environmental sequencing data. Methods Ecol Evol 4:914–919.

42. Nilsson RH, Larsson KH, Taylor AFS, Bengtsson-Palme J, Jeppesen TS, Schigel D, Kennedy P, Picard K, Glöckner FO, Tedersoo L, Saar I, Kõljalg U, Abarenkov K. 2019. The UNITE database for molecular identification of fungi: handling dark taxa and parallel taxonomic classifications. Nucleic Acids Res 47:D259–D264.

43. Quast C, Pruesse E, Yilmaz P, Gerken J, Schweer T, Yarza P, Peplies J, Glöckner FO. 2013. The SILVA ribosomal RNA gene database project: improved data processing and web-based tools. Nucleic Acids Res 41:D590–D596.

44. Zhang Z, Schwartz S, Wagner L, Miller W. 2000. A greedy algorithm for aligning DNA sequences. J Comput Biol 7:203–214.

45. Boylen E, Rideout JR, Dillon MR, Bokulich NA, Abnet CC, Al-Ghalith GA, Alexander H, Alm EJ, Arumugam M, Asnicar F, Bai Y, Bisanz JE, Bittinger K, Brejnrod A, Brislawn CJ, Brown CT, Callahan BJ, Caraballo-Rodriguez AM, Chase J, Cope EK, Da Silva R, Dorrestein

PC, Douglas GM, Durall DM, Duvallet C, Edwardson CF, Ernst M, Estaki M, Fouquier J, Gauglitz JM, Gibson DL, Gonzalez A, Gorlick K, Guo J, Hillmann B, Holmes S, Holste H, Huttenhower C, Huttley GA, Janssen S, Jarmusch AK, Jiang L, Kaehler BD, Kang KB, Keefe CR, Keim P, Kelley ST, Knights D, Koester I, Kosciolek T, Kreps J, Langille MGI, Lee J, Ley R, Liu YX, Loftfield E, Lozupone C, Maher M, Marotz C, Martin BD, McDonald D, McIver LJ, Melnik AV, Metcalf JL, Morgan SC, Morton JT, Naimey AT, Navas-Molina JA, Nothias LF, Orchanian SB, Pearson T, Peoples SL, Petras D, Preuss ML, Pruesse E, Rasmussen LB, Rivers A, Robeson MS II, Rosenthal P, Segata N, Shaffer M, Shiffer A, Sinha R, Song SJ, Spear JR, Swafford AD, Thompson LR, Torres PJ, Trinh P, Tripathi A, Turnbaugh PJ, Ul-Hasan S, van der Hooft JJJ, Vargas F, Vázquez-Baeza Y, Vogtmann E, von Hippel M, Walters W, Wan Y, Wang M, Warren J, Weber KC, Williamson CHD, Willis AD, Xu ZZ, Zaneveld JR, Zhang Y, Zhu Q, Knight R, Caporaso JG. 2018. QIIME 2 : Reproducible, interactive, scalable, and extensible microbiome data science. PeerJ Prepr 6e27295v2 https//doi.org/107287/peerj.preprints27295v2.

46. McDonald D, Clemente JC, Kuczynski J, Rideout JR, Stombaugh J, Wendel D, Wilke A, Huse S, Hufnagle J, Meyer F, Knight R, Caporaso JG. 2012. The Biological Observation Matrix (BIOM) format or: How I learned to stop worrying and love the ome-ome. Gigascience 1:1–6.

47. Katoh K, Standley DM. 2013. MAFFT multiple sequence alignment software version 7: Improvements in performance and usability. Mol Biol Evol 30:772–780.

48. Price MN, Dehal PS, Arkin AP. 2010. FastTree 2--approximately maximum-likelihood trees for large alignments. PLoS One 5:e9490.

49. Faith DP. 1992. Conservation evaluation and phylogenetic diversity. Biol Conserv 61:1–10.

50. Pinheiro JC, Bates DM. 2004. Mixed-effects models in S and S-Plus. Springer, New York, USA.

51. Bates D, Mächler M, Bolker BM, Walker SC. 2015. Fitting linear mixed-effects models using lme4. J Stat Softw 67:1–48.

52. Kuznetsova A, Brockenhoff PB, Christensen RHB. 2017. lmerTest: Tests in linear mixed effects models. R package version 2.0-32.

53. Warton DI. 2011. Regularized sandwich estimators for analysis of high-dimensional data using generalized estimating equations. Biometrics 67:116–123.

54. Wang Y, Naumann U, Wright ST, Warton DI. 2012. Mvabund - an R package for model-based analysis of multivariate abundance data. Methods Ecol Evol 3:471–474.

55. Forstner C, Orton TG, Skarshewski A, Wang P, Kopittke PM, Dennis PG. 2019. Graphene oxide affects soil bacterial and fungal diversity even at parts-per-trillion concentrations GenBank https://dataview.ncbi.nlm.nih.gov/object/PRJNA515098.

Table 1 Summary of multivariate GLM post-hoc results computed using mvabund highlighting differences in bacterial community composition between treatments relative to the controls within each time point.

	P value
Day 7 GO Low	<0.001***
Day 7 GO Medium	<0.001***
Day 7 GO High	<0.001***
Day 7 Graphite Low	<0.001***
Day 7 Graphite Medium	<0.001***
Day 7 Graphite High	<0.001***
Day 14 GO Low	0.140
Day 14 GO Medium	0.003**
Day 14 GO High	0.020*
Day 14 Graphite Low	<0.001***
Day 14 Graphite Medium	<0.001***
Day 14 Graphite High	0.006**
Day 30 GO Low	0.001**
Day 30 GO Medium	<0.001***
Day 30 GO High	0.021*
Day 30 Graphite Low	<0.001***
Day 30 Graphite Medium	<0.001***
Day 30 Graphite High	0.001**

Table 2 Summary of multivariate GLM post-hoc results computed using mvabund highlighting differences in fungal community composition between treatments relative to the controls.

	P value
GO Low	0.001**
GO Medium	0.005**
GO High	0.005**
Graphite Low	0.002**
Graphite Medium	0.001**
Graphite High	0.001**

Figure Legends

Fig. 1 The numbers of predicted bacterial and fungal OTUs (Chao1) after 7, 14 and 30 days by treatment. The error bars represent standard deviations. None of the treatments differed significantly from the controls.

Fig. 2 Principal coordinate analysis (PCoA) ordination illustrating differences in the composition of bacterial communities in control, and graphite and GO amended soils over time. The ellipses represent standard deviations. The three panels, representing different time points, derive from a single ordination that included all samples. Each time point is shown separately to avoid over-cluttering. The arrows for each treatment move from low, through medium, to high dose. They highlight that there was not a consistent direction of change in community composition with increasing GO or graphite dose.

Fig. 3 Heatmap of the relative abundances of 49 bacterial OTUs that differed significantly from the control in at least one treatment combination. The asterisks highlight which treatments differ significantly from the controls on each day ($P < 0.05$*, $P < 0.01$**, $P < 0.001$***). Each column of the heatmap represents the mean relative abundance of each treatment (n = 3). The bubble-plot on the left summarizes the number (circle size) of GO or graphite doses that an OTU responded to relative to the controls, and of these how many manifested as increases or decreases in relative abundance (circle color). The numbers below the bubble plot and heatmap show the total numbers of significant responses to a particular treatment relative to the control within the same day. The OTU IDs are consistent throughout the manuscript. The phylum of each OTU is

indicated by the colors on the left of the heatmap and the affiliations associated with each color are shown at the bottom.

Fig. 4 Principal coordinate analysis (PCoA) ordination illustrating differences in the composition of fungal communities in control, and graphite and GO amended soils over time. The ellipses represent standard deviations. The three panels, representing different time points, derive from a single ordination that included all samples. Each time point is shown separately to avoid over-cluttering. On day 30, one of the control samples (PCO1 = 1.2, PCO2 = -0.07) is beyond the plotted area. The arrows for each treatment move from low, through medium, to high dose. They highlight that there was not a consistent direction of change in community composition with increasing GO or graphite dose.

Fig. 5 Heatmap of the relative abundances of 16 fungal OTUs that differed significantly from the control in at least one treatment combination. The asterisks highlight which treatments differ significantly from the controls on each day ($P < 0.05$*, $P < 0.01$**, $P < 0.001$***). Each column of the heatmap represents the mean relative abundance of each treatment (n = 9). The bubble-plot on the left summarizes the number (circle size) of GO or graphite doses that an OTU responded to relative to the controls, and of these how many manifested as increases or decreases in relative abundance (circle color). The numbers below the bubble plot and heatmap show the total numbers of significant responses to a particular treatment relative to the control within the same day. The OTU IDs are consistent throughout the manuscript. The phylum and class of each OTU is indicated by the colors on the left of the heatmap and the affiliations associated with each color are shown at the bottom.

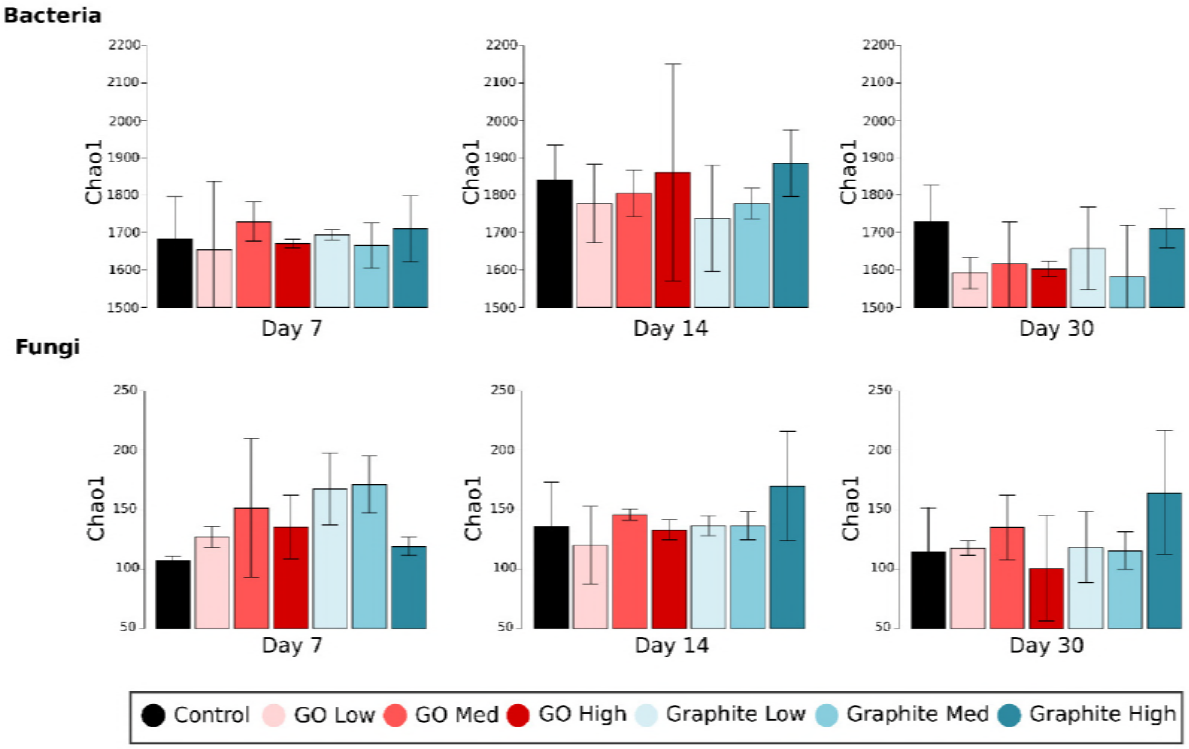

Fig. 1 The numbers of predicted bacterial and fungal OTUs (Chao1) after 7, 14 and 30 days by treatment. The error bars represent standard deviations. None of the treatments differed significantly from the controls.

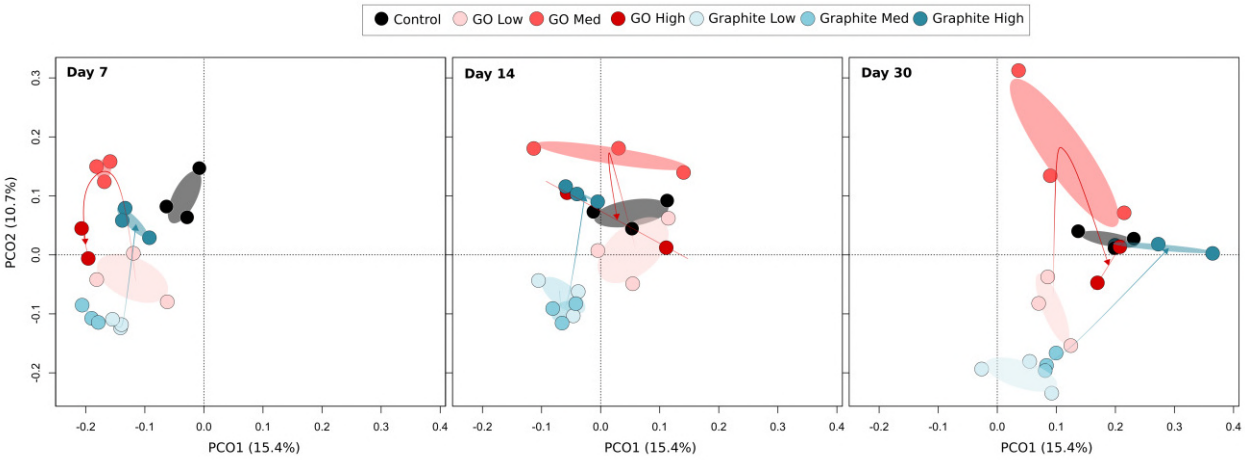

Fig. 2 Principal coordinate analysis (PCoA) ordination illustrating differences in the composition of bacterial communities in control, and graphite and GO amended soils over time. The ellipses represent standard deviations. The three panels, representing different time points, derive from a single ordination that included all samples. Each time point is shown separately to avoid over-cluttering. The arrows for each treatment move from low, through medium, to high dose. They highlight that there was not a consistent direction of change in community composition with increasing GO or graphite dose.

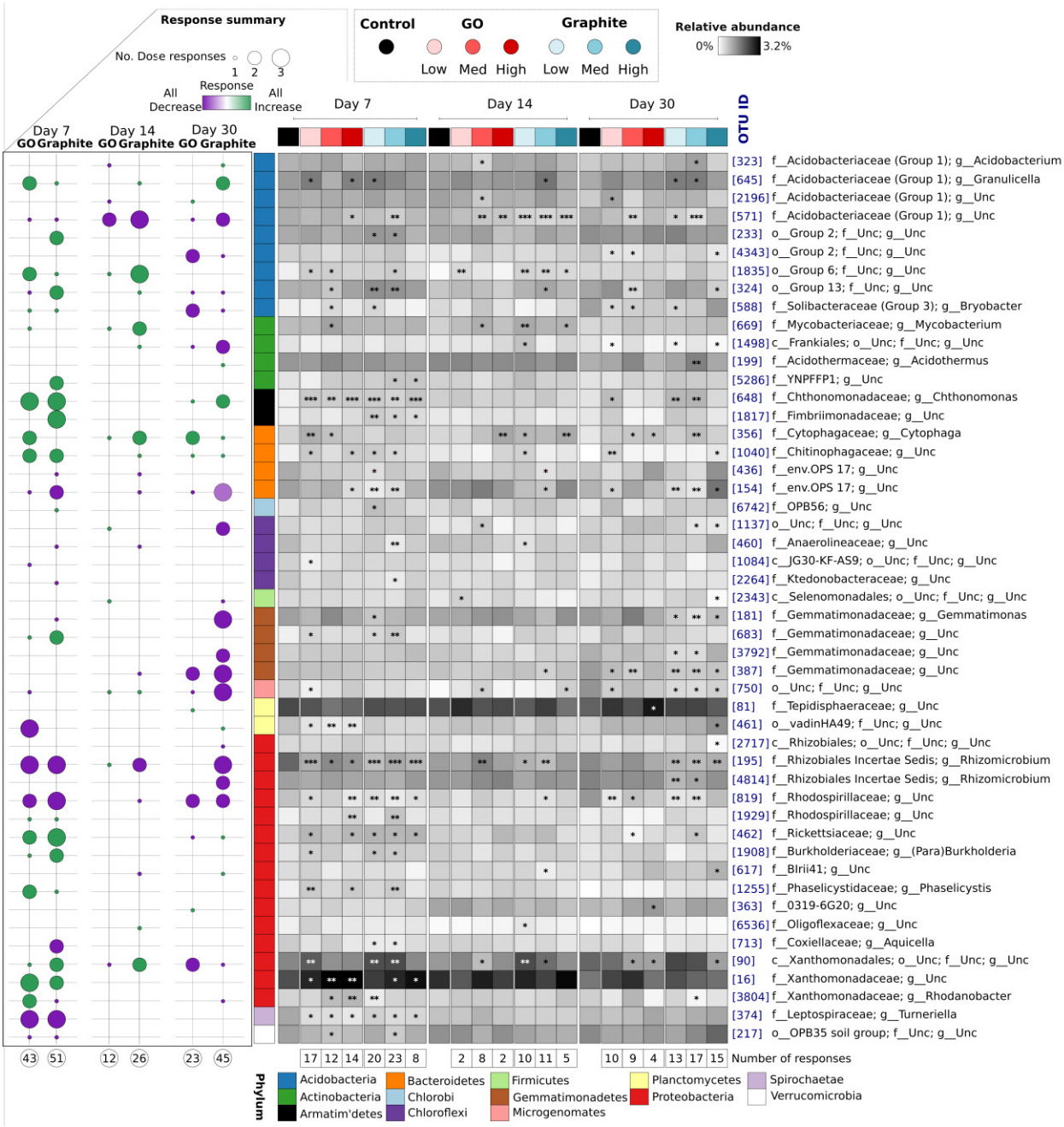

Fig. 3 Heatmap of the relative abundances of 49 bacterial OTUs that differed significantly from the control in at least one treatment combination. The asterisks highlight which treatments differ significantly from the controls on each day ($P < 0.05$*, $P < 0.01$**, $P < 0.001$***). Each column

of the heatmap represents the mean relative abundance of each treatment (n = 3). The bubble-plot on the left summarizes the number (circle size) of GO or graphite doses that an OTU responded to relative to the controls, and of these how many manifested as increases or decreases in relative abundance (circle color). The numbers below the bubble plot and heatmap show the total numbers of significant responses to a particular treatment relative to the control within the same day. The OTU IDs are consistent throughout the manuscript. The phylum of each OTU is indicated by the colors on the left of the heatmap and the affiliations associated with each color are shown at the bottom.

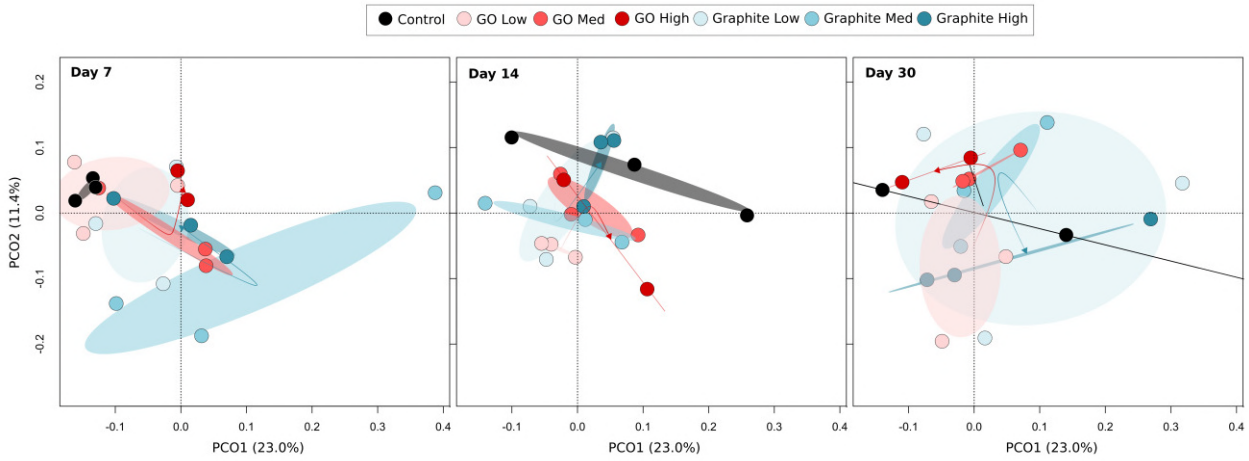

Fig. 4 Principal coordinate analysis (PCoA) ordination illustrating differences in the composition of fungal communities in control, and graphite and GO amended soils over time. The ellipses represent standard deviations. The three panels, representing different time points, derive from a single ordination that included all samples. Each time point is shown separately to avoid over-cluttering. On day 30, one of the control samples (PCO1 = 1.2, PCO2 = -0.07) is beyond the plotted area. The arrows for each treatment move from low, through medium, to high dose. They highlight that there was not a consistent direction of change in community composition with increasing GO or graphite dose.

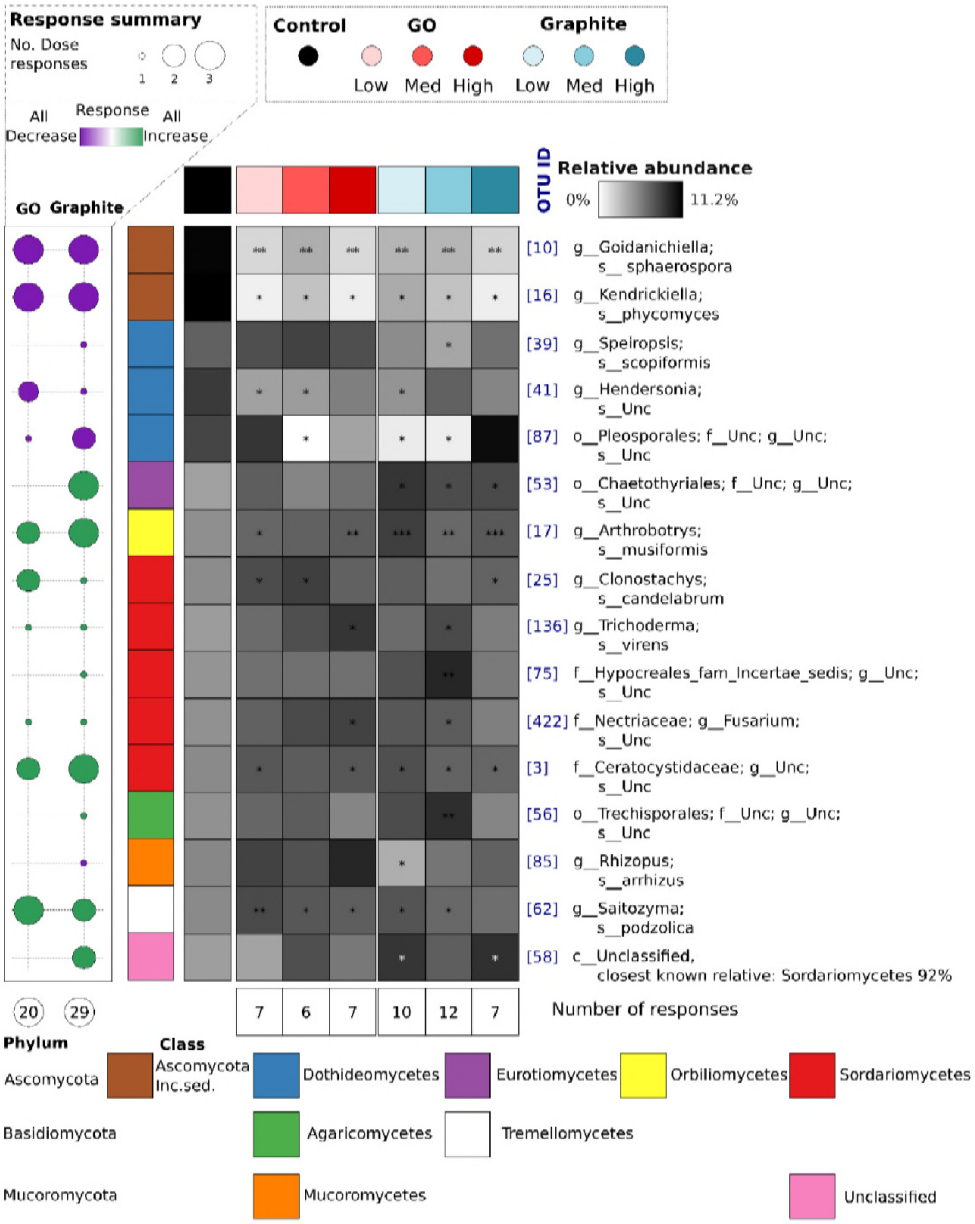

Fig. 5 Heatmap of the relative abundances of 16 fungal OTUs that differed significantly from the control in at least one treatment combination. The asterisks highlight which treatments differ significantly from the controls on each day ($P < 0.05$*, $P < 0.01$**, $P < 0.001$***). Each column of the heatmap represents the mean relative abundance of each treatment (n = 9). The bubble-plot on the left summarizes the number (circle size) of GO or graphite doses that an OTU responded

to relative to the controls, and of these how many manifested as increases or decreases in relative abundance (circle color). The numbers below the bubble plot and heatmap show the total numbers of significant responses to a particular treatment relative to the control within the same day. The OTU IDs are consistent throughout the manuscript. The phylum and class of each OTU is indicated by the colors on the left of the heatmap and the affiliations associated with each color are shown at the bottom.